RSC Advances

PAPER

View Article Online
View Journal | View Issue

Cite this: RSC Adv., 2017, 7, 12998

Efficiency and stability enhancement of inverted perovskite solar cells *via* the addition of metal nanoparticles in the hole transport layer†

G. Kakavelakis,*[ab] K. Alexaki,[cd] E. Stratakis[bc] and E. Kymakis*[a]

Received 8th January 2017
Accepted 17th February 2017

DOI: 10.1039/c7ra00274b

rsc.li/rsc-advances

In this work, the addition of different types (Au, Ag and Al) of metal nanoparticles (NPs) in the PEDOT:PSS hole transport layer of inverted perovskite solar cells was systematically studied. The Ag and Au NP incorporation led to the highest power conversion efficiency improvement, while the Al NP-based devices showed significantly improved stability compared to the pristine one. Efficiencies exceeding 13.5% were demonstrated.

Introduction

Organometal halide perovskite semiconductors have attracted a significant amount of attention in the field of optoelectronic devices in recent years.[1] Due to their extraordinary optical and electronic properties,[2–4] hybrid perovskite-based semiconductors have attracted great interest presenting tremendous potential to be established as an efficient photovoltaic technology. Therefore, hybrid metal halide based perovskite solar cells (PSCs) have reached power conversion efficiencies (PCEs) of more than 22% in a few years,[5,6] directly competing with the already established technologies.

One of the main advantages of PSCs compared to commercial photovoltaics is that all the device layers can be deposited at room temperature, through a solution process, making this technology able to be also established as a low cost and flexible photovoltaic technology. However, since the high PCEs have been reached using a mesoporous structure[7] that requires thermal treatment of ~450 °C for TiO_2 sintering, the development of PSCs in flexible substrates is impossible. Alternatively, the fabrication of PSCs using the inverted structure fulfils all the requirements towards room temperature production on flexible substrates, however the PCEs are significantly lower,[8,9] and alternative routes needs to be adopted to tackle this tradeoff. Further improvements are still likely through enhanced electronic properties of the crystalline perovskite thin films and the interfacial layers.

Despite the acceptable PCEs and the low fabrication cost of inverted PSCs on flexible and ultra-lightweight substrates, their commercialization requires also high levels of stability. In this context, the long-term operational instability of PSCs,[10,11] need to be effectively resolved. Thus, the high sensitivity of lead halide perovskites to ambient conditions (humidity) is still significant bottleneck towards the commercialization of the PSCs.

One strategy to improve the PCE of thin film solar cells, including PSCs, could be by optically engineering the device to maximize light coupling into the active layer. For this purpose, metal nanoparticles (NPs) that confine resonant photons by an induced coherent surface plasmonic oscillation of their conduction band electrons,[12] the so-called localized surface plasmon resonance (LSPR), at which a significant enhancement of light absorption and scattering takes place.[13] Furthermore, it has been previously demonstrated that the addition of metal NPs in organic solar cells can also improve the charge extraction and the stability of the device.[14,15] In addition, the facile tunability of their optical properties by modifying the type, size, shape, and surrounding materials of NPs has shown high potential as an optical engineering tool in thin-film optoelectronic devices.[16] However, only a few studies in the literature report the use of metal NPs in normal or mesostructured PSCs,[17–22] with no direct evidences regarding the metal NPs beneficial role in inverted PSCs structure.

In this letter, we report the addition of noble metal NPs in the hole transport layer (HTL) of planar inverted perovskite solar cells. In particular, we studied the beneficial role of adding individually gold (Au), silver (Ag) and aluminum NPs (Al) in the poly(3,4-ethylenedioxythiophene) polystyrene sulfonate (PEDOT:PSS) HTL. It is shown that, in all cases, the addition of NPs gives rise to enhanced electron extraction and in turn device efficiency, while the addition of Al NPs resulted in

[a]Center of Materials Technology and Photonics, Electrical Engineering Department, Technological Educational Institute (TEI) of Crete, Heraklion 71004, Crete, Greece. E-mail: Kakavelakis@staff.teicrete.gr; kymakis@staff.teicrete.gr

[b]Department of Materials Science and Technology, University of Crete, Heraklion, 710 03 Crete, Greece

[c]Institute of Electronic Structure and Laser (IESL), Foundation for Research and Technology-Hellas (FORTH), Heraklion, Greece

[d]Physics Department, University of Crete, Heraklion, 710 03 Crete, Greece

† Electronic supplementary information (ESI) available. See DOI: 10.1039/c7ra00274b

a significant enhancement of the device stability. More important, we show that the simultaneous addition of Ag and Al NPs in the HTL, gives rise to a hysteresis-free inverted PSC with efficiency of ~12.4% and high levels of ambient stability.

Experimental

Details on the device fabrication[23] and the preparation of metal NPs dispersions by laser ablation can be found in our previous publications.[24–28] Specifically, following the preparation of NPs *via* ultrashort pulsed laser ablation of the respective metal targets in ethanol, the as prepared Au, Ag and Al NPs, with average diameters of ~10, ~20 and ~30 nm respectively (see Fig. S1†), were dispersed in proper concentration inside the PEDOT:PSS and stirred for at least two hours. Afterwards, the solutions with and without metal NPs were spin coated onto the indium tin oxide (ITO) coated glass substrates, following by annealing the films for 15 minutes at 120 °C in ambient atmosphere. After a mixture solution of 1 : 3 ratio of $PbCl_2$-: CH_3NH_3I in *N*,*N*-dimethylformamide (DMF) solvent was spin coated onto the different NPs-doped PEDOT:PSS layers at 4000 rpm. The precursor films were annealed at 100 °C for 75 minutes in ambient conditions to form the mixed halide hybrid perovskite ($CH_3NH_3PbI_{3-x}Cl_x$) based absorber. A 2% phenyl-C61-butyric acid methyl ester (PCBM) in chlorobenzene solution was coated onto the perovskite layers at 1000 rpm. After that, 0.04% polyelectrolyte poly[(9,9-bis(30-(*N*,*N*-dimethylamino)propyl)-2,7-fluorene)-*alt*-2,7-(9,9-dioctylfluorene)] (PFN) in methanol was spin-coated on PCBM layer at 2000 rpm. Finally, the devices were transferred to vacuum chamber for Al electrode evaporation. The detailed characterization process of the devices can be found elsewhere.[23]

Results

The $CH_3NH_3PbI_{3-x}Cl_x$ perovskite film characterization on ITO/PEDOT:PSS substrates can be found in previous a publication.[23] To assess the viability of metal NPs in the planar inverted PSCs, devices with architecture of ITO/PEDOT:PSS/$CH_3NH_3PbI_{3-x}Cl_x$/PCBM/PFN/Al, with and without the addition of Au, Ag and Al NPs in the PEDOT:PSS HTL were fabricated. Fig. 1a displays the current density–voltage (*J*–*V*) curves of the pristine and the Au, Ag, and Al NPs-doped PEDOT:PSS PSCs using the $CH_3NH_3PbI_{3-x}Cl_x$ as the solar absorber. An important enhancement in the short-circuit current density (J_{sc}) was observed for the Au and Ag NPs-doped devices, accompanied by a satisfactory enhancement in the fill factor (FF) compared to the pristine device, while the open circuit voltage (V_{oc}) remained constant. On the other hand, a smaller enhancement was observed for the Al NPs-doped devices J_{sc} while the V_{oc} remained almost the same. The highest PCE was observed for the Ag-NPs doped device, with a record value of ~13%. Contrary highest PCE values for the pristine, Au and Al NPs-doped devices were ~11.5%, ~12.5% and ~12% respectively. As a result, a ~13% enhancement in PCE was obtained for the Ag NPs-doped devices compared to the pristine one (Table 1 and Fig. 1a). After systematic investigation of the effect of the different NPs concentration in PEDOT:PSS on PSCs performance, we concluded that a concentration of ~5% v/v NPs was the optimum for each case, in terms of PCE. In Table S1† (ESI) can be found the optimization experiments of NPs concentration inside the PEDOT:PSS layer in terms of the device performance. Fig. S2† also present the *J*–*V* characteristics plotted for both the forward and reverse scans, showing almost no discrepancy among the device parameters, indicating the absence of the hysteresis effect of the devices tested. It is also important to mention, that a smaller series resistance (R_s) measured for the Ag doped PSCs (6.18 Ω cm^2) compared to the reference device (7.46 Ω cm^2), explaining also the important improvement in the FF value of the former. The lower PCE enhancement of Al doped PSCs and the higher measured R_s, can be ascribed to the fact that, in such NPs an ultra-thin oxide layer is formed, right after their preparation through laser ablation in liquids, reducing in this way the NP conductivity.[28]

To confirm the enhancement of the J_{sc} in the NP-based devices, the external quantum efficiency (EQE) spectra of $CH_3NH_3PbI_{3-x}Cl_x$ PSCs, with and without the addition of the different NPs in PEDOT:PSS were measured (Fig. 1b). It is clear, that for all the NPs doped devices the EQE spectra exhibits

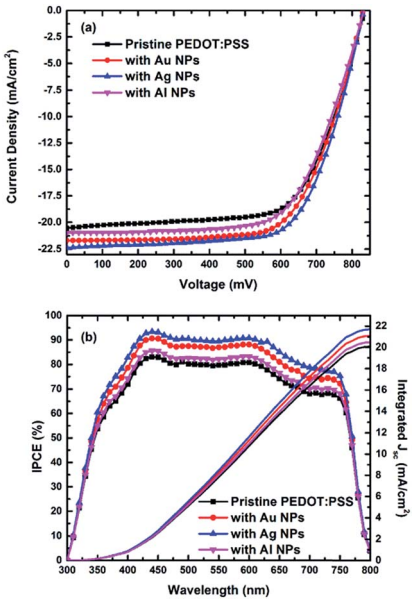

Fig. 1 (a) The *J*–*V* curves of perovskite solar cells doped with and without Au, Ag and Al NPs and measured under AM 1.5G (100 mW cm^{-2}) illumination. (b) External quantum efficiency (EQE) spectra of the same devices.

Table 1 Photovoltaic characteristics of PSCs with different NPs embedded in the PEDOT:PSS HTL

NPs	J_{sc} (mA cm^{-2})	V_{oc} (mV)	FF (%)	PCE (%)	R_s (Ω cm^2)
No	20.55 ± 1.04	838 ± 9	65.83 ± 0.57	11.33 ± 0.81	7.46
Au	21.69 ± 0.98	837 ± 10	67.03 ± 0.45	12.18 ± 0.78	7.14
Ag	22.37 ± 1.02	838 ± 10	67.64 ± 0.62	12.68 ± 0.86	6.18
Al	20.94 ± 0.89	839 ± 11	65.97 ± 0.54	11.58 ± 0.76	8.69

a broad increase in the entire active spectrum compared to the pristine device. The highest increase is observe for the Ag NPs doped PSCs. Additionally, we measured the absorption spectra of the $CH_3NH_3PbI_{3-x}Cl_x$ on ITO/PEDOT:PSS substrates with and without the addition of the different metallic NPs in the HTL, showing almost no discrepancy among the different samples (Fig. S3†). This indicates that the mechanism of efficiency enhancement cannot be attributed to plasmonic contribution. Another point to be noted, is that the integrated J_{sc} from EQE is less than 3% different from the actual measured J_{sc} values (Table 1), indicating good accuracy of our electrical measurements. Furthermore, Fig. S4† provides the transmittance spectra of pristine PEDOT:PSS and Au, Ag and Al NPs doped PEDOT:PSS films, spin-coated on ITO substrates which gives important information regarding the parasitic absorption/reflection of the metal particles. Compared with the pristine, Au, Ag and Al doped devices showed slightly lower transmittance in the range of 300–400 and 400–500 nm and 500–600 respectively, because of their LSPR. If we combine the transmittance measurements with the IPCE we can conclude that tradeoff between charge extraction and parasitic reflection in the front surface of the cell is significantly improved with the addition of the NPs in the HTL of the PSCs.

To get an insight into the charge extraction properties of the photogenerated carriers from the hybrid perovskite to the different NPs-doped HTLs, the samples' steady state photoluminescence (PL) spectra were measured and analysed as shown in Fig. 2a. It is evident that, the $CH_3NH_3PbI_{3-x}Cl_x$ film deposited on Ag doped PEDOT:PPS shows the most significant PL quenching, compared to the pristine and the Au and Al NPs doped devices, proving that the Ag NPs doping has successfully enhanced the rate of carrier extraction at the HTL/perovskite interface.[3,29] The PL results further support our findings from the *I–V* and EQE spectra, suggesting that upon the addition of Ag NPs in the HTL, the J_{sc} was significantly enhanced due to improvement in hole extraction.

To better understand the origin of the performance enhancement in the NP-based PSCs, the *I–V* characteristics were measured in sandwich cells composed by ITO/HTL/Au, with pristine PEDOT:PSS or PEDOT:PSS doped with Au, Ag and Al used as HTLs (Fig. 2b). The DC (direct current) conductivity (σ_0) can be determined from the slope of *I–V* plot, using the equation

$$I = \sigma_0 A d^{-1} V,$$

where A is the area of sample (0.04 cm^2) and d is the thickness of sample (40 nm), respectively.[29] The conductivity of pristine PEDOT:PSS was 0.599 ± 0.004 mS cm^{-1}, whereas the Ag doped PEDOT:PSS film presented ~4 fold higher conductivity (2.412 ± 0.001 mS cm^{-1}). As a result, it is expected that the photogenerated charge carriers in $CH_3NH_3PbI_{3-x}Cl_x$ based absorber are more efficiently transported to the Ag NPs-doped PEDOT:PSS HTL than to the pristine PEDOT:PSS. The higher conductance of the Ag NPs based HTL justifies the observed PL quenching, originating from the improved charge extraction from the perovskite towards the HTL. The Au and Al NPs-doped devices conductance follow the same trend as that shown by the of *I–V* and EQE measurements; *i.e.* the σ_0 of Au doped device (2.087 ± 0.001 mS cm^{-1}) was significant higher compared to the Al doped device (0.897 ± 0.007 mS cm^{-1}).

Apart from the study of the NPs effect on the PCE, we also studied their effect on the device stability (Fig. 3).

It has been recently demonstrated that the PEDOT:PSS based PSCs are very unstable when exposure to ambient conditions with constant light soaking and thus rapidly degrade.[30] By comparing the degradation rate of the pristine and the NPs-doped devices, we observed an entirely different trend from that observed for the respective device efficiencies. In particular, the degradation rate of the pristine and the high efficiency NPs-doped devices, *i.e.* the Ag and Au doped cells, was almost the same with a slight increase in the case of the NPs doped devices. On the contrary, the addition of Al NPs in the PEDOT:PSS HTL seems to slow down the

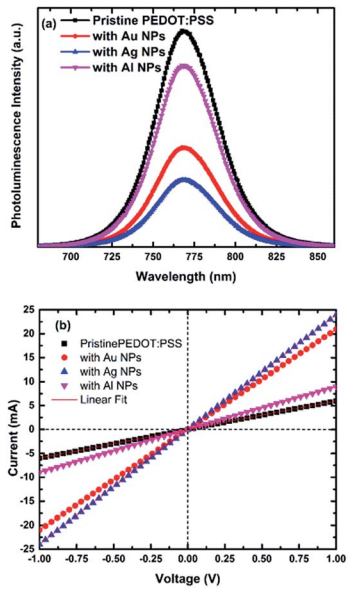

Fig. 2 (a) Photoluminescence (PL) spectra (excitation at 543 nm) of glass/PEDOT:PSS and NPs:PEDOT:PSS/$CH_3NH_3PbI_{3-x}Cl_x$ substrates. (b) *I–V* characteristics of ITO/PEDOT:PSS/Au and ITO/NPs:PEDOT:PSS/Au devices.

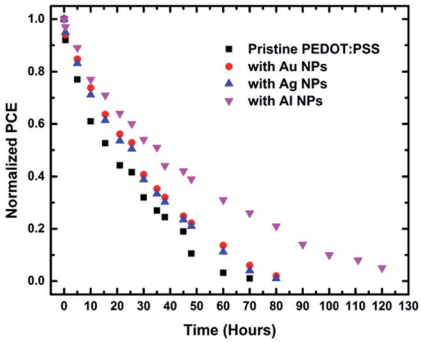

Fig. 3 Evolution of normalized PCE of PEDOT:PSS and NPs:PEDOT:PSS HTLs based PSCs under continuous solar illumination in ambient conditions (~50% RH).

degradation rate by a factor of ~2. This trend has already observed before in organic photovoltaic cells incorporating Al NPs,[31] attributed to the fact that Al NPs retard the degradation of the PEDOT:PSS buffer layer in the presence of moisture. This mechanism was not observed here upon doping with Ag or Au NPs. Similar to this study, the degradation of the PSCs was monitored in ambient conditions with high levels of humidity (>50% relative humidity). Therefore, the improved stability observed in the case of Al NPs-doped devices can be directly interpreted by the same mechanism(s) identified in our previous study[31] on organic solar cells.

In order to have a clear view regarding the mechanism responsible for the higher lifetime of PSCs doped with metal NPs and in particular those incorporating Al NPs into the PEDOT:PSS HTL, we monitored the XRD spectra evolution of the hybrid perovskite deposited on the different PEDOT:PSS doped substrates under continuous solar illumination in ambient conditions. For this purpose, we have collected the respective XRD spectra before and after degradation for 24 hours. Fig. 4a presents the spectra for pristine samples; one can observe almost identical XRD patterns among the different samples, indicating that the perovskite absorber is not affected in the initial stage from the presence of the metal NPs in the HTL. On the other hand, when we stressed the different films with continuous solar illumination (Fig. 4b), we obtained completely different trends. In particular, for the NPs-free thin film, we observed the formation of a new high intensity peak at ~12.80°, which is directly correlated with the degradation of the perovskite crystal structure due to the formation of PbI_2 moieties into the crystal.[32] In the cases of Ag and Au-doped HTL based layers, the perovskite seems to follow almost the same trend with the NPs free sample, with a slight decreased intensity of the PbI_2 characteristic peak, which is directly correlated with the slightly slower degradation rate that such devices showed with respect to the undoped device. On the other hand, in case of the Al-doped HTL based layers, the perovskite structure appeared to become less degraded, since the intensity of the PbI_2 peak is less pronounced. This is again in full agreement with the respective PCE degradation rate of the devices. It is highly possible that Al NPs may be further oxidized from the residual water present into the PEDOT:PSS layer, considering that aluminum is very reactant in the presence of water and becomes oxidized immediately. As a result the amount of water molecules that reach the perovskite layer becomes limited.[31]

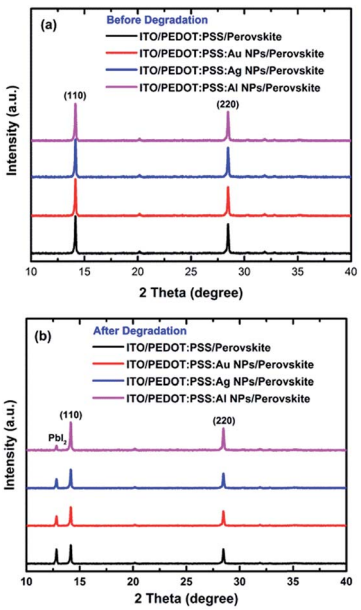

Fig. 4 XRD patterns of perovskite deposited in pristine and the different NPs doped PEDOT:PSS substrates (a) before and (b) after the degradation.

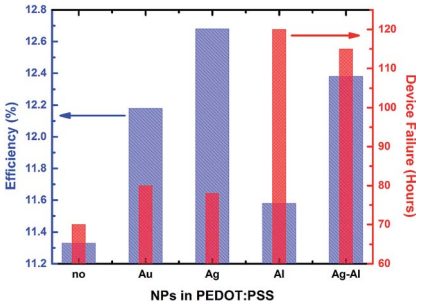

Fig. 5 General overview of the PCE and degradation trend upon different type of NP incorporation inside the HTL.

Thus, to further extend this approach, we fabricated inverted PSCs with the addition of both Ag and Al in the PEDOT:PSS HTL, to study their affect in performance and stability at the same time. As it can be clearly observed in Fig. S5a and b† the efficiency of Ag–Al doped devices was almost the same with the Ag doped ones with a slight decrease in J_{sc}, while the degradation rate of such device was at the same levels of the highly stable Al doped device. Thus, by simply adding both Al and Ag NPs, with equal concentration, and using exactly the same fabrication conditions, we were able to fabricate PSCs with high efficiency and ambient stability. In order to have a more general view of our results, in Fig. 5 we plotted the trend of PCE and degradation rate using the pristine and the different doped HTLs. It can be easily understood that by introducing both Ag and Al we were able to obtain high efficiency and stability at the same time.

Conclusions

In summary, metal NPs were successfully added in the PEDOT:PSS HTL of fully solution processable planar inverted PSCs. The introduction of Ag and Au NPs in PEDOT:PSS resulted in a significant PCE enhancement of PSCs, while, the addition of Al NPs in the PEDOT:PSS significantly extended device stability upon prolonged illumination under ambient conditions. The introduction of both Ag and Al NPs in the HTL of the device resulted simultaneous and significant enhancement of the device efficiency and stability compared to the pristine PSC. Our work opens new pathways for efficiency and stability optimization of PSCs, perovskite light emitting diodes, perovskite photodetectors and other novel perovskite-based devices, using low cost, solution processable noble metal NPs, deposited and

treated at low temperature, providing the opportunity for the development of high efficient devices in flexible, ultra-light substrates.

Acknowledgements

This work was financially supported by the Research Projects for Excellence IKY/Siemens.

Notes and references

1 S. D. Stranks and H. J. Snaith, *Nat. Nanotechnol.*, 2015, **10**, 391.
2 N. K. Kumawat, M. N. Tripathi, U. Waghmare and D. Kabra, *J. Phys. Chem. A*, 2016, **120**, 3917.
3 S. D. Stranks, G. E. Eperon, G. Grancini, C. Menelaou, M. J. P. Alcocer, T. Leijtens, L. M. Herz, A. Petrozza and H. J. Snaith, *Science*, 2013, **342**, 341.
4 Y. H. Lee, J. Luo, R. Humphry-Baker, P. Gao, M. Grätzel and M. K. Nazeeruddin, *Adv. Funct. Mater.*, 2015, **25**, 3925.
5 A. Kojima, K. Teshima, Y. Shirai and T. Miyasaka, *J. Am. Chem. Soc.*, 2009, **131**, 6050.
6 NREL*Best Researchs-Cell Photovoltaic Efficiency Chart*, 2016.
7 M. Saliba, T. Matsui, J.-Y. Seo, K. Domanski, J.-P. Correa-Baena, M. K. Nazeeruddin, S. M. Zakeeruddin, W. Tress, A. Abate, A. Hagfeldt and M. Grätzel, *Energy Environ. Sci.*, 2016, **9**, 1989.
8 P. Docampo, J. M. Ball, M. Darwich, G. E. Eperon and H. J. Snaith, *Nat. Commun.*, 2013, **4**, 2761.
9 J. H. Heo, H. J. Han, D. Kim, T. K. Ahn and S. H. Im, *Energy Environ. Sci.*, 2015, **8**, 1602.
10 A. Mei, X. Li, L. Liu, Z. Ku, T. Liu, Y. Rong, M. Xu, M. Hu, J. Chen, Y. Yang, M. Grätzel and H. Han, *Science*, 2014, **345**, 295.
11 T. A. Berhe, W.-N. Su, C.-H. Chen, C.-J. Pan, J.-H. Cheng, H.-M. Chen, M.-C. Tsai, L.-Y. Chen, A. A. Dubaleb and B.-J. Hwang, *Energy Environ. Sci.*, 2016, **9**, 323.
12 X. Huang, S. Neretina and M. A. El-Sayed, *Adv. Mater.*, 2009, **21**, 4880.
13 H. Chen, L. Shao, Q. Li and J. Wang, *Chem. Soc. Rev.*, 2013, **42**, 2679.
14 G. Kakavelakis, I. Vangelidis, A. Heuer-Jungemann, A. G. Kanaras, E. Lidorikis, E. Stratakis and E. Kymakis, *Adv. Energy Mater.*, 2016, **6**, 1501640.
15 J.-L. Wu, F.-C. Chen, Y.-S. Hsiao, F.-C. Chien, P. Chen, C.-H. Kuo, M. H. Huang and C.-S. Hsu, *ACS Nano*, 2011, **5**, 959.
16 K. L. Kelly, E. Coronado, L. L. Zhao and G. C. Schatz, *J. Phys. Chem. B*, 2003, **107**, 668.
17 M. Saliba, W. Zhang, V. M. Burlakov, S. D. Stranks, Y. Sun, J. M. Ball, M. B. Johnston, A. Goriely, U. Wiesner and H. J. Snaith, *Adv. Funct. Mater.*, 2015, **25**, 5038.
18 W. Zhang, M. Saliba, S. D. Stranks, Y. Sun, X. Shi, U. Wiesner and H. J. Snaith, *Nano Lett.*, 2013, **13**, 4505.
19 Z. Yuan, Z. Wu, S. Bai, Z. Xia, W. Xu, T. Song, H. Wu, L. Xu, J. Si, Y. Jin and B. Sun, *Adv. Energy Mater.*, 2015, **5**, 1500038.
20 W. R. Erwin, H. F. Zarick, E. M. Talbert and R. Bardhan, *Energy Environ. Sci.*, 2016, **9**, 1577.
21 Z. Lu, X. Pan, Y. Ma, Y. Li, L. Zheng, D. Zhang, Q. Xu, Z. Chen, S. Wang, B. Qu, F. Liu, Y. Huang, L. Xiao and Q. Gong, *RSC Adv.*, 2015, **5**, 11175.
22 M. He, X. Pang, X. Liu, B. Jiang, Y. He, H. J. Snaith and Z. Lin, *Angew. Chem.*, 2016, **55**, 4280.
23 G. Kakavelakis, T. Maksudov, D. Konios, I. Paradisanos, G. Kioseoglou, E. Stratakis and E. Kymakis, *Adv. Energy Mater.*, 2016, DOI: 10.1002/aenm.201602120.
24 G. Kakavelakis, E. Stratakis and E. Kymakis, *RSC Adv.*, 2013, **3**, 16288.
25 G. Kakavelakis, E. Stratakis and E. Kymakis, *Chem. Commun.*, 2014, **50**, 5285.
26 E. Kymakis, G. D. Spyropoulos, R. Fernandes, G. Kakavelakis, A. G. Kanaras and E. Stratakis, *ACS Photonics*, 2015, **2**, 714.
27 B. Paci, G. Kakavelakis, A. Generosi, J. Wright, C. Ferrero, E. Stratakis and E. Kymakis, *Sol. Energy Mater. Sol. Cells*, 2017, **159**, 617.
28 E. Stratakis, M. Barberoglou, C. Fotakis, G. Viau, C. Garcia and G. A. Shafeev, *Opt. Express*, 2009, **17**, 12650.
29 B.-X. Chen, H.-S. Rao, W.-G. Li, Y.-F. Xu, H.-Y. Chen, D.-B. Kuang and C.-Y. Su, *J. Mater. Chem. A*, 2016, **4**, 5647.
30 H. Chen, Y. Hou, C. E. Halbig, S. Chen, H. Zhang, N. Li, F. Guo, X. Tang, N. Gasparini, I. Levchuk, S. Kahmann, C. O. Ramirez Quiroz, A. Osvet, S. Eigler and C. J. Brabec, *J. Mater. Chem. A*, 2016, **4**, 11604.
31 M. Sygletou, G. Kakavelakis, B. Paci, A. Generosi, E. Kymakis and E. Stratakis, *ACS Appl. Mater. Interfaces*, 2015, **7**, 17756.
32 S. N. Habisreutinger, T. Leijtens, G. E. Eperon, S. D. Stranks, R. J. Nicholas and H. J. Snaith, *Nano Lett.*, 2014, **14**, 5561.

